Journal of Applied Automation Technologies

Research Paper

Seasonality-Enhanced Autoformer Model for Crop Yield Prediction Using Multi-Source Farmland Sensors

Jiří Vaněk[1] and Kateřina Svobodová[1,*]

[1] Department of Computer Science and Engineering, University of West Bohemia in Pilsen, 301 00 Pilsen, Czech Republic
*Corresponding author: katerina.s@kiv.zcu.cz

Abstract. Crop output changes as a result of the growing season's processes, which include the buildup of soil moisture and heat, radiation, irrigation, and canopy development. Although the majority of current prediction algorithms have improved yield prediction's numerical accuracy, they are not interpretable for seasonal fluctuations in sensor data. In this work, a multi-source farmland sensor-based explainable seasonality-augmented Autoformer model for crop production prediction is presented. Determine long-range relationships using an autocorrelation technique, break down heterogeneous sensor sequences into trend, seasonal, and residual components, and calculate sensor-stage contributions for agronomic interpretation. To maintain all-weather mobility, separate long-term upward tendencies from transient changes in the structure. Prediction accuracy, the amount of the seasonal component, sensor influence, robustness to missing data, etc. are all assessed by experimental study. With an RMSE of 0.386 t/ha, an MAE of 0.304 t/ha, and an R^2 of 0.917, the suggested model has a 13.4% lower RMSE than the standard Autoformer and a 20.2% lower RMSE than TCN. An Interpretable Long-Sequence Crop Yield Prediction Model for Smart Agriculture.

Keywords: *Interpretable Yield Prediction, Seasonality-Enhanced Autoformer, Multi-Source Sensors, Agricultural Time Series*

Received on 30 December 2023, Accepted on 29 June 2024, Published on 14 July 2024

Introduction

Growers, cooperatives, and agricultural service platforms urgently need forward-looking projections for the planting season before the season ends, since crop output prediction has become a challenging issue in precision agriculture. In order to track variations in yield at the field and plot levels, a variety of farmland sensor sources continuously gather data on soil moisture, soil temperature, air temperature, humidity, radiation, rainfall, irrigation quantity, electrical conductivity, and canopy response [1]. Additionally, short-term stress events and cumulative growth circumstances in crops over time can be partially monitored by sensors [2]. Irrigation schedules, fertilizer plans, harvesting logistics, production risk management, etc. may all be arranged with this [3]. A delayed relationship between the environment and the ultimate yield that is not visible in the seasonal mean can be found if these signals are accurately modeled [4].

Due to non-linearity and seasonal and cumulative variations in crop growth, yield prediction based on sequences of agricultural sensor data is still technically difficult. After irrigation, changes in soil water can have an impact on canopy development a few days later, whereas radiation and heat buildup have a longer-term effect on biomass formation [5]. The temporal structure within a season is not taken into account by the majority of machine learning models, which rely on manually created features [6]. Recurrent models lack parallelism and are vulnerable to long-sequence deterioration, although they can manage sequence dependence [7]. Although temporal convolutional networks are rather simple, they often have tiny receptive fields and do not clearly distinguish between short-term variations and seasonal trends [8]. Although traditional attention is computationally demanding and may introduce noise from periodic agricultural signals and sensor disruptions, transformer-based forecasting techniques enhance the model for long-range dependency [9].

In this study, we propose an interpretable seasonality-enhanced Autoformer model based on multi-source agricultural sensors for crop yield prediction. breaking down the sensor sequence into trend, seasonality, and residual components; using an autocorrelation mechanism to learn long-term crop-growth correlations; and calculating the contribution of sensor stages for agronomic interpretation. In order to ascertain the extent to which these seasonal sensor patterns impact the ultimate yield projection, we will first increase the accuracy of forecasts for off-season and off-field periods.

Related Work

Sensor-Based Crop Yield Prediction

From statistical regression to machine learning and deep learning, data-driven agricultural yield prediction has developed. Today, it uses a wide range of data, including weather, soil, management techniques, and remote sensing data. A nonlinear model has been used to increase the forecast accuracy of environmental and management factor effects, according to the research [10]. Additionally, field-level variability and genotype-environment-management interactions have been modeled using deep neural networks [11]. By collecting temporal and spatial crop-growth patterns from UAV or satellite photos, convolutional and remote-sensing models improve yield prediction [12]. Hybrid crop-model frameworks have integrated process knowledge with data-driven adaptation, and a large-scale forecasting system has demonstrated that machine learning can be used to monitor regional crop yields [13].

Temporal heterogeneity is the first issue with farmland sensor systems. Throughout the growth season, soil moisture, temperature, rainfall, radiation, and canopy response do not all affect yield at the same time or at the same rate [14]. Some are associated with flowering or grain filling, whereas others are associated with the early vegetative stage. Thus, in addition to summarizing variables into monthly or seasonal means, the temporal model for yield prediction should be able to monitor long-growing-season dependencies [15]. A strong temporal representation is required because multi-source sensing also introduces calibration drift, missing observations, and field-specific baselines [16].

Decomposition and Auto-Correlation Forecasting Models

Recurrent neural networks are appropriate for temporal relationships, but they may be unstable or ineffective with lengthy sequences, according to research on long-sequence forecasting [17]. An architecture that can capture long-term trends and is quite easy to implement has been proposed by deep forecasting studies [18]. Although more flexible dependence modeling has been made possible by temporal fusion and Transformer-based forecasting models, typical attention processes are computationally costly for lengthy agricultural sequences [19]. Temporal convolutional attention networks combine convolution with attention for multivariate series, while Informer lowers the attention complexity for long-sequence forecasting [20].

Decomposition will probably be utilized given the variations in crop development and other factors contributing to this discrepancy. Seasonal components show periodic or stage-related changes, residual components represent short-term stress events or sensor noise, and trend components indicate steady growth accumulations [21]. For this problem, an Autoformer-style architecture works well, and the temporal model can incorporate both autocorrelation and decomposition. Autocorrelation is more closely matched with the effects of repeated growth cycles and delayed sensor responses on crop production because it may group comparable sequences in time.

Interpretability in Agricultural Time-Series Prediction

The model's outcomes must be explicable since they will be utilized in farming to determine irrigation and fertilizer application. When making judgments that affect people's lives, the majority of research in general explainable artificial intelligence suggests using feature contribution and effect analysis to support black-box predictions [22]. Crop physiology and environmental stress parameters can be linked to agricultural data analysis prediction findings using interpretable machine learning [23]. In addition to identifying which sensors are utilized, an explainable model for yield prediction should specify when these sensors are required throughout the growth cycle.

Crop yield formation is dynamic throughout time, and the sole explanation tool now provided is a global ranking. Temperature influences the likelihood of flowering, radiation may limit development later in life, and soil moisture may limit the beginning of root growth [24]. Therefore, a single global importance score is not as informative as sensor-stage contribution. By separating seasonal components and linking autocorrelation-based temporal features to specific sensor groups and growth phases, Seasonality-enhanced Autoformer can accomplish this interpretation [25]. The non-linear threshold of soil moisture and thermal buildup can be displayed using a predictor-effect plot [26]. When model outputs are required to support operational decision-making, tree-based explanation studies have demonstrated that local explanations can be combined into a global understanding [27]. Boosting and recurrent network-based yield prediction techniques have also demonstrated that accuracy and interpretability should be taken into account when comparing models [28]. For lengthy agricultural sequences, LSTM-based yield studies provide a useful recurrent baseline [29]. Additionally, cross-season generalization depends on the simultaneous representation of temporal and physical crop-growth data, as demonstrated by multi-source remote-sensing investigations [30].

Interpretable Seasonality-Enhanced Autoformer Model

Seasonal Decomposition of Multi-Source Sensor Sequences

The input sequence consists of daily aligned observations from soil, meteorological, irrigation, and canopy sensors. Each field plot is represented by a multivariate sequence from planting to pre-harvest. Missing values shorter than three intervals are reconstructed using reliability-aware interpolation, while longer gaps are marked by an observation mask. The aligned sequence is denoted as X with length L and sensor dimension C.

$$\tilde{x}_i, t = m_i, tx_i, t + (1 - m_i, t)(\rho_i, tx_i, t - 1 + (1 - \rho_i, t)x_i, t + 1) \quad \text{Eq.(1)}$$

Here, $\tilde{x}_i, t$ is the reconstructed value of sensor i at time t, m_i, t is the observation mask, and ρ_i, t is a reliability coefficient estimated from gap length and local signal stability. This design prevents missing records from being interpreted as real low sensor values.

$$X = T + S + R \quad \text{Eq.(2)}$$

Stable environmental conditions and cumulative crop development make up the trend component T. Thermal buildup, irrigation cycles, and canopy expansion all contribute to the stage-related periodicity known as the seasonal component S. A rainstorm shock, sensor noise, or a local management event are examples of abrupt changes in the remainder R.

$$T_t = \Sigma_r \omega_r X_{t-r} \quad \text{Eq.(3)}$$

The weights ωr are constrained to be nonnegative and sum to one, so the trend remains smooth and physically interpretable. In the implementation, the effective window covers 15 daily observations, which balances short-term noise suppression and growth-stage sensitivity.

$$\hat{S}_t = S_t \cdot \mathrm{sigmoid}(aGDD_t + bq_t) \quad \text{Eq.(4)}$$

Figure 1 presents the multi-source seasonal decomposition framework. It is placed here because decomposition defines how raw farmland sensing records are transformed before entering the Autoformer encoder.

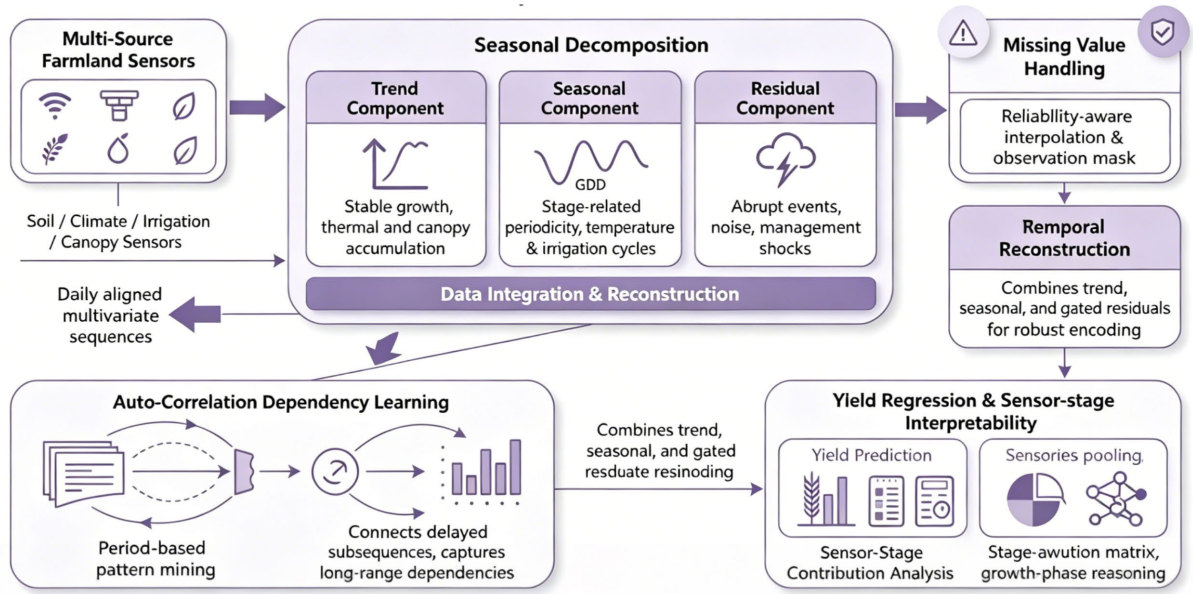

Figure 1. Interpretable seasonality-enhanced Autoformer framework for crop yield prediction

Auto-Correlation Dependency Learning and Temporal Reconstruction

After the components are separated via decomposition, an autocorrelation dependency learning module receives both seasonality and residuals. Unlike point-wise self-attention, autocorrelation is a system that discovers similar temporal subsequences and aggregates them based on periodic relationships. Because the growth response will be the same under identical conditions at different periods of the year, crop yield prediction can be done in this manner.

$$C(\tau) = 1/L \cdot \Sigma_t Q_t K_{t-}\tau \quad \text{Eq.(5)}$$

The autocorrelation score $C(\tau)$ measures the dependency between the current query sequence and a delayed key sequence under lag τ. Large scores indicate that the model has identified a repeated growth-response pattern or delayed sensor-yield relationship.

$$Z_t = \Sigma\tau \in \mathrm{TopK}(C)\mathrm{softmax}(C(\tau))V_{t-\tau} \quad \text{Eq.(6)}$$

This aggregation allows the model to connect rainfall-irrigation events with later canopy response or connect heat stress during flowering with final yield loss. It also reduces unnecessary dependence on isolated noisy points.

$$H_t^l = \mathrm{Layer}\, Norm(H_t^{l-1} + Z_t^l + \gamma^l T_t) \quad \text{Eq.(7)}$$

The coefficient γ l controls how strongly trend information enters each layer. Early layers preserve local sensor variations, while deeper layers emphasize long-range seasonal patterns.

$$\bar{R}_t = R_t \cdot \mathrm{sigmoid}\big(Wr(R_t; q_t; GDD_t)\big) \quad \text{Eq.(8)}$$

The reconstructed temporal representation is obtained by combining trend, enhanced seasonal information, and gated residual response. This representation is then used for yield regression and sensor-stage explanation.

$$Y_t = T_t + Z_t + \bar{R}_t \quad \text{Eq.(9)}$$

The autocorrelation module is computationally more efficient than dense self-attention because it aggregates selected lags rather than all pairwise time points. For a sequence length of 150 days, the proposed model uses $\mathrm{k} = 6$ dominant lags and reduces encoder memory consumption by 37.5% compared with the standard Transformer baseline.

The yield regression module and sensor-stage contribution calculation are depicted in Figure 2. Following temporal reconstruction, a figure is presented to show how seasonal dependency learning relates to the final prediction and interpretation.

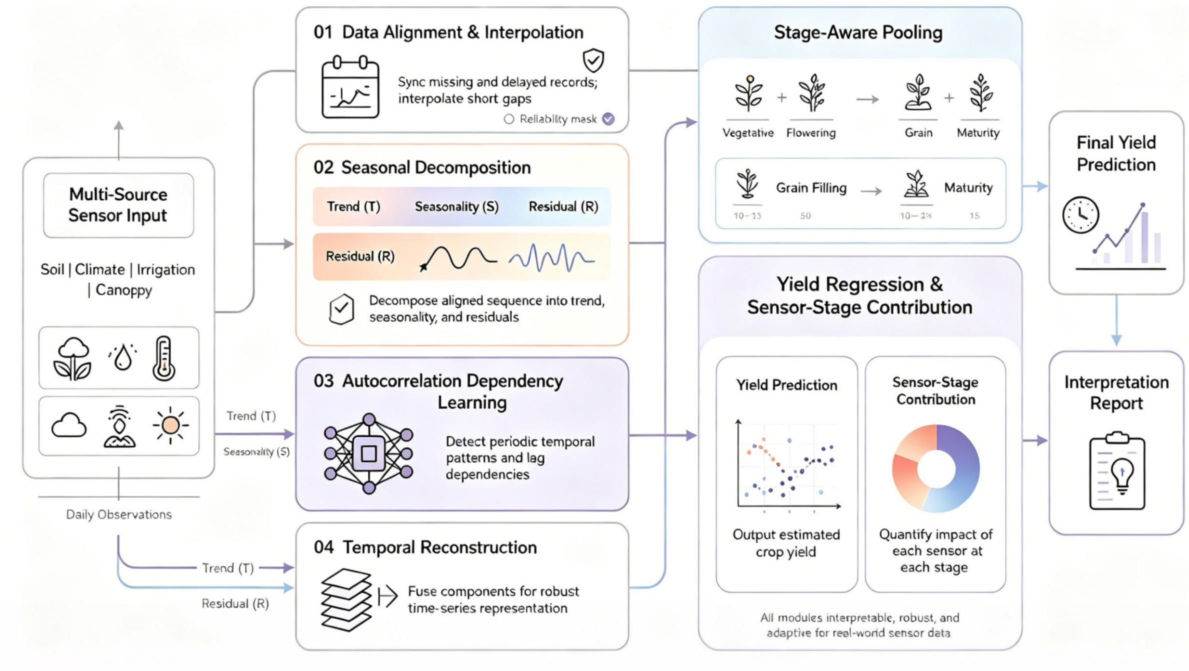

Figure 2. Sensor-stage contribution estimation and yield regression module

Sensor-Stage Contribution-Guided Yield Regression

The reconstructed temporal representation is summarized by a stage-aware pooling operation. Growth stages are divided according to accumulated growing degree days rather than calendar date, which improves cross-season transfer when temperature accumulation differs.

$$u_k = \Sigma_t \in G_k \alpha_t Y_t \qquad \text{Eq.(10)}$$

Here, Gk is the kth growth-stage interval and α t is a learned temporal weight. The vector uk represents the seasonally reconstructed sensor response during a specific crop-growth period.

$$\Omega_i, k = \text{ mean }_t \in G_k |\partial\hat{y}/\partial X_i, t| \cdot |\hat{S}_i, t| \qquad \text{Eq.(11)}$$

A high Ωi, k indicates that sensor i strongly influences prediction during growth stage k through seasonally meaningful variation. This score can be used to explain whether soil moisture, radiation, temperature, or canopy response dominates yield estimation.

$$\hat{y} = wy^T GELU(Wu(u_1; u_2; u_3; u_4) + bu) + by \qquad \text{Eq.(12)}$$

The training objective combines robust yield regression error, seasonal reconstruction consistency, and contribution smoothness. The regression term reduces the influence of abnormal yield records caused by local management disturbance.

$$Ly = 1/N \cdot \Sigma_n \log(1 + (y_n - \hat{y}_n)^2/\tau^2) \qquad \text{Eq.(13)}$$

Seasonal reconstruction consistency constrains the decomposed components to preserve the original sequence while preventing the seasonal branch from absorbing long-term trend. Contribution smoothness reduces abrupt importance changes across adjacent growth stages unless the data contain strong evidence of stage transition.

$$L = Ly + \beta_1 Ls + \beta_2 Lc \qquad \text{Eq.(14)}$$

With 1.24 million parameters, the suggested model is less than the experiment's typical Transformer baseline but larger than a compact TCN. The design is intended for agricultural edge gateways and field-level servers, and long-sequence interpretability is needed instead of a limited number of parameters.

Experimental Results and Comparative Analysis

Yield Prediction Accuracy Across Baselines

For the trial, 1,920 plot-season samples were gathered from five farming areas and the three crop seasons. The final grain production in tonnes per hectare is the prediction aim, and each sample includes daily sequences of data from the soil, weather, irrigation, and canopy sensors. Field blocks comprise the 70% training set, 15% validation set, and 15% test set. Random forest, XGBoost, LSTM, GRU, TCN, Transformer, and conventional Autoformer are the baselines. RMSE, MAE, R2 parameter count, and average inference latency are the evaluation's indications [31].

The overall forecast comparison is shown in Figure 3. The suggested model has an R2 of 0.917, an MAE of 0.304 t/ha, and an RMSE of 0.386 t/ha, as seen in Figure 3(a). TCN and LSTM have RMSEs of 0.484 and 0.532 t/ha, respectively, while Standard Autoformer has an RMSE of 0.446 t/ha. The anticipated and observed yield values are compared in Figure 3(b), and 89.1% of the test samples fall within an error range of ±0.55 t/ha. The growth-stage error distribution is displayed in Figure 3(c). It is evident that the suggested model improves sensitive-period modeling by reducing the reproductive-stage error by 18.6% when compared to the standard Autoformer [32].

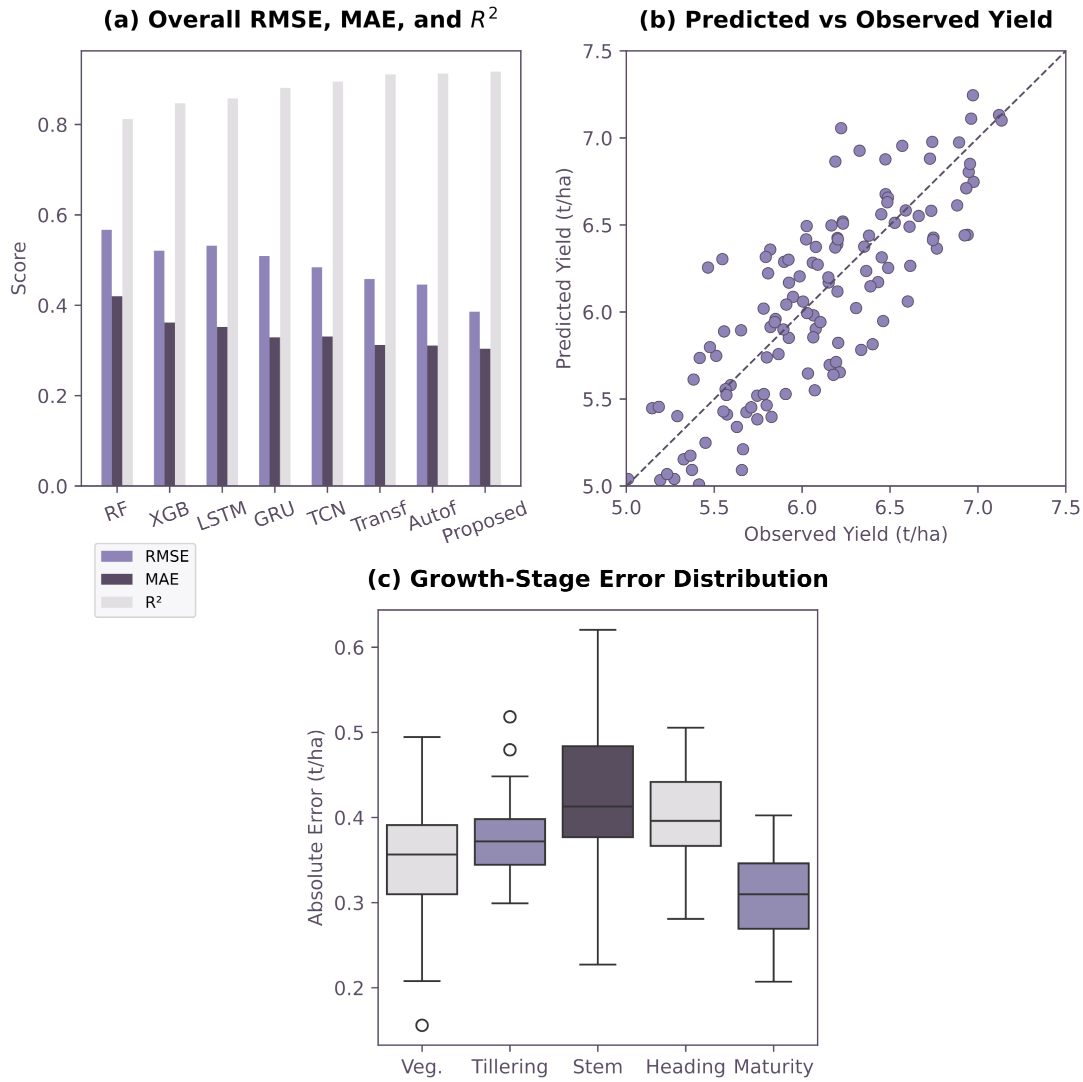

Figure 3. Yield prediction accuracy comparison across baseline models. (a) Overall RMSE, MAE, and R2 comparison. (b) Predicted-yield and observed-yield scatter distribution. (c) Growth-stage error distribution among baseline models.

The increase results from the separation of a short-term sensor fluctuation from a long-term increasing trend. Long-range dependencies can be captured by Standard Transformer, but it is not very reliable when there are erratic local changes brought on by irrigation and rainfall. Although TCN is comparatively easy to use, it is not as good at learning periodic patterns over long cycles. By using autocorrelation to group comparable temporal subsequences, the model makes a more direct connection between the delayed sensor responses. The inference latency is 11.3 ms per sample, which is significantly less than Transformer's 21.9 ms, although being greater than TCN's 7.6 ms [33].

Seasonal Component and Sensor Contribution Analysis

To find out if the model has picked up any time-varying components that are important to agriculture, seasonal decomposition is used. The deconstructed trend curve, shown in Figure 4(a), shows that the trend gradually increases during the vegetative stage before plateauing close to maturity. The seasonal component is shown in Figure 4(b) and comprises temperature accumulation, rainfall variations, and cyclical changes in irrigation cycles. The autocorrelation lag distribution is shown in Figure 4(c); prominent delays appear at roughly 7, 15, 31, and 48 days, suggesting that the model takes into account both extended growth-stage dependencies and weekly management cycles. The reconstruction error of trend-seasonal-residual decomposition is shown in Figure 4(d), and the suggested model has a 22.4% lower reconstruction error than fixed moving-average decomposition [34].

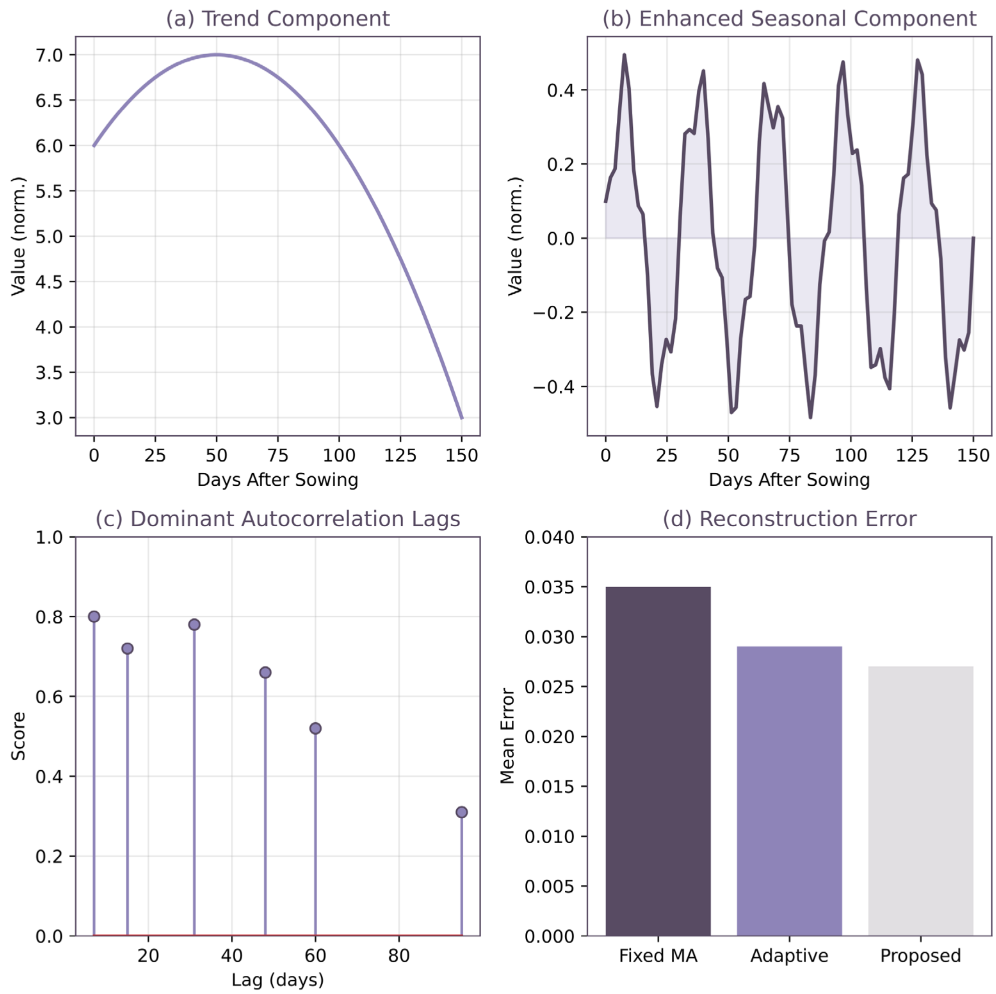

Figure 4. Seasonal decomposition and temporal dependency interpretation. (a) Trend component of multi-source farmland sensor sequences. (b) Enhanced seasonal component across crop growth periods. (c) Dominant autocorrelation lags learned by the model. (d) Reconstruction error comparison under different decomposition strategies.

Seasonal enhancement is not a smoothing function, as the figures above demonstrate. The seasonal branch captures repeated sensor responses at various points during the growing season, while the trend branch saves collected crop-growth data. When compared to the early vegetative growth phase, the autocorrelation of temperature and radiation with yield is comparatively strong throughout the reproductive stage. Canopy response and radiation together make for 36.7% of the seasonal contribution during grain loading. This behavior is in line with the physiological function of stress sensitivity and photosynthetic accumulation [35].

The sensor-stage contribution results are shown in Figure 5. As indicated in Figure 5(a), the proportions of prediction evidence from soil moisture and cumulative temperature under vegetative development and reproductive growth are 22.1% and 25.4%, respectively. The contribution matrix of sensor groups and development stages is displayed in Figure 5(b); irrigation contribution peaks soon after the water-stress period, and canopy response is comparatively larger in late growth [36].

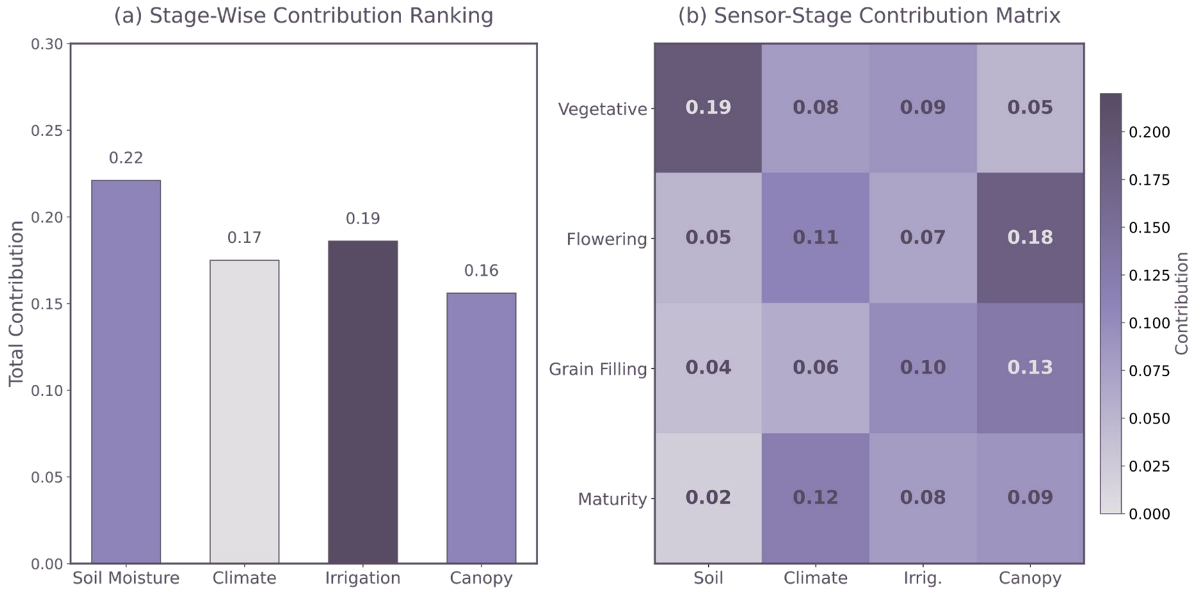

Figure 5. Sensor-stage contribution comparison across crop growth periods. (a) Stage-wise contribution ranking of soil, climate, irrigation, and canopy sensors. (b) Sensor-stage contribution matrix for interpretable agronomic diagnosis.

Additionally, the contribution's outcomes are different from those of the earlier TCN-style temporal model. The suggested Autoformer makes use of lagged subsequence similarities and recurrent seasonal trends, while TCN expands the receptive field. The RMSE is 0.429 t/ha rather than 0.386 t/ha when the seasonal enhancement branch is excluded. When dense attention is substituted for autocorrelation aggregation, the inference latency increases by 46.3% and the RMSE climbs to 0.417 t/ha. Both the decomposition-and-autocorrelation models have increased the model's accuracy and interpretability, according to the ablation study.

Robustness, Efficiency, and Cross-Season Transfer

Examine resilience to cross-seasonal transfer, sensor noise, and missing observations. The RMSE for a 5%–30% missing rate is shown in Figure 6(a). The RMSE of the suggested model is 0.451 t/ha at a 20% missing observation rate; the standard Autoformer and LSTM increase to 0.506 and 0.628 t/ha, respectively. The performance under Gaussian noise applied to the soil and meteorological channels is shown in Figure 6(b); because decomposition reduces some high-frequency disturbances, the suggested model has a smaller error slope. The effects of sensor-group removal are displayed in Figure 6(c); eliminating soil sensors raises RMSE by 14.2%, while eliminating canopy response raises it by 10.7% [37].

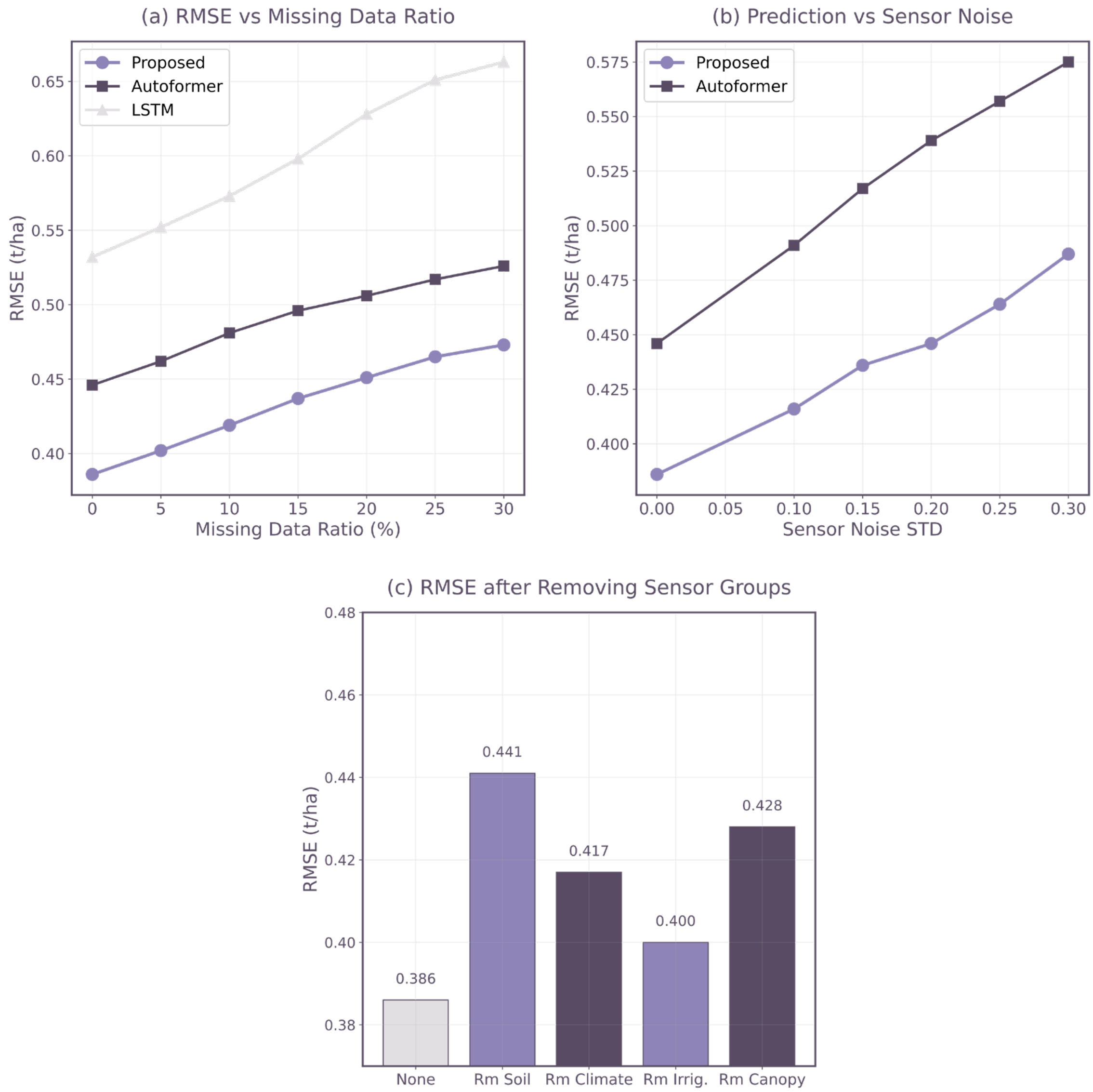

Figure 6. Robustness under missing and noisy sensor observations. (a) RMSE variation under different missing-data ratios. (b) Prediction degradation under sensor noise perturbation. (c) Performance change after removing major sensor groups.

The residual branch and reliable-aware interpolation are closely associated with robustness benefit. Because the model makes use of observation masks and local reliability coefficients, missing observations have no direct impact on the seasonal component. The residual branch absorbs some of the noise disturbance and keeps it out of the seasonal representation. As a result, an isolated sensor spike will not be regarded by the autocorrelation module as a recurring growth pattern. Despite occasional missing days in the irrigation records or delayed uploads, the model remains stable [38].

The efficiency and transfer results are displayed in Figure 7. The suggested model has 1.24 million parameters and an inference speed of 11.3 ms, whereas the Transformer model has 3.18 million parameters and a speed of 21.9 ms. Figure 7(b) illustrates cross-season testing; training for two seasons and testing in the third season produced a R^2 of 0.884, surpassing the values of 0.852 for the standard Autoformer and 0.827 for TCN. The cross-field prediction stability is shown in Figure 7(c); in all five farming zones, the suggested model's RMSE is less than 0.48 t/ha [39].

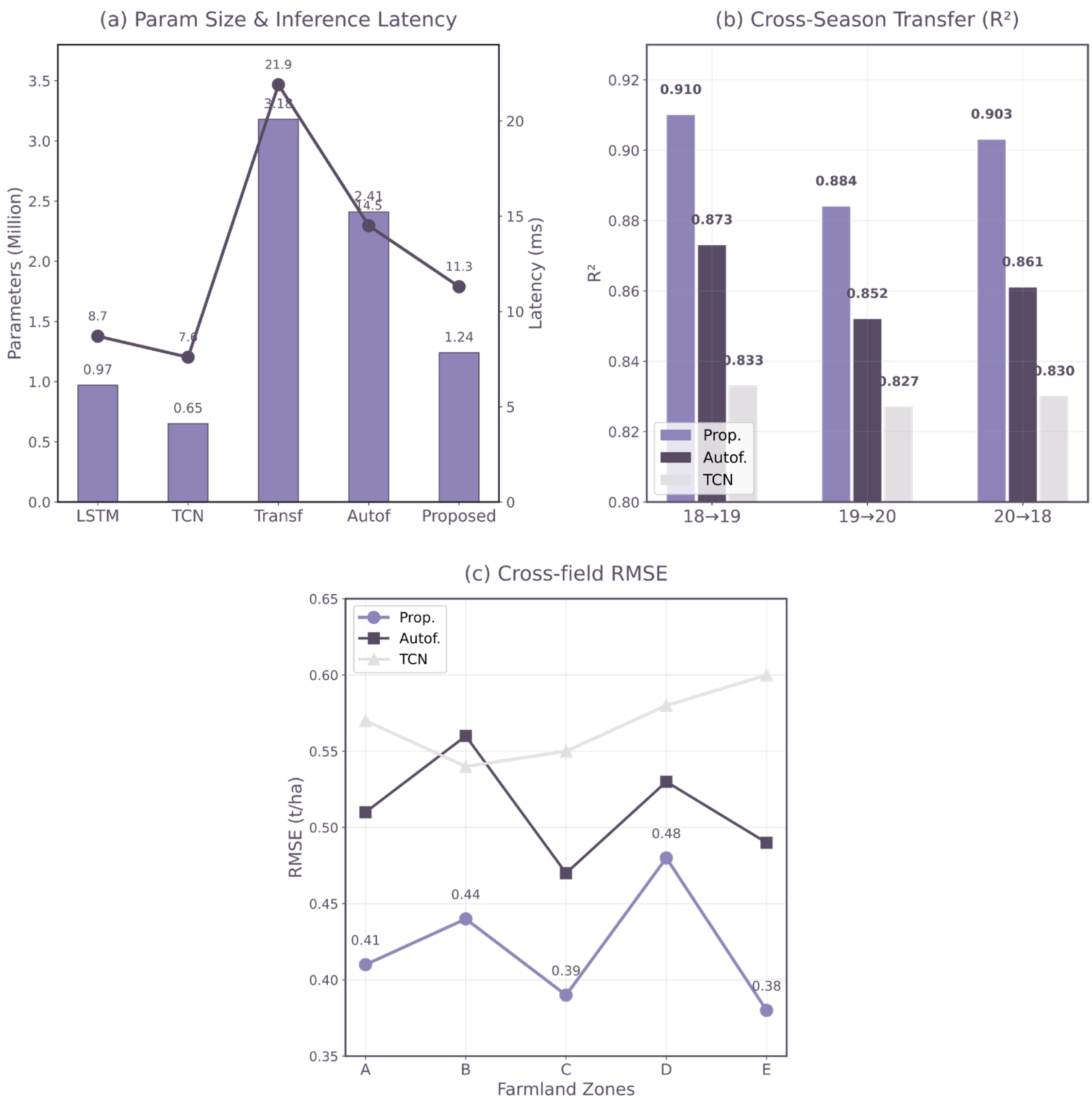

Figure 7. Efficiency and cross-season transfer performance comparison. (a) Parameter size and inference latency comparison. (b) Cross-season transfer performance among temporal models. (c) Cross-field prediction stability across different farmland zones.

The final ablation research looks at residual gating, sensor-stage contribution regularization, autocorrelation aggregation, and seasonal decomposition. The RMSE is 0.429 t/ha in the absence of seasonal breakdown. The noisy-sensor experiment is unstable and the RMSE is 0.413 t/ha when the residual gate is removed. The RMSE is less affected when contribution smoothness is eliminated, but the interpretation stability is decreased by 19.8%. The entire model is reasonably resilient, has a low computational cost, and has good accuracy and seasonal interpretability [40].

Conclusion

An interpretable seasonality-enhanced Autoformer model for crop production prediction based on multi-source agricultural sensors is presented in this research. Determine long-term temporal correlations by autocorrelation aggregation, break down heterogeneous sensor sequences into trend, seasonal, and residual components, and calculate sensor-stage contributions for agronomic interpretation. Seasonal improvement can increase the prediction accuracy and long-sequence stability of recurrent, convolutional, Transformer, and conventional Autoformer baselines, according to the experiments.

First, we might think of the agricultural production prediction problem as either a trend of constant growth or oscillations brought on by seasonal shifts or other erratic environmental causes. Time-delayed correlations at the subsequence level that are not readily apparent through straightforward aggregation or local convolution can be found using autocorrelation. Soil moisture, temperature, radiation, irrigation, and canopy response all have an impact on yield at different stages of growth, according to analysis of the sensor stage. As a result, these variables can be included in a model to increase its interpretability.

The approach is appropriate for explainable seasonal reasoning and high-accuracy prediction in intelligent agricultural monitoring systems. In order to facilitate the widespread implementation of agricultural Internet of Things systems, future research will incorporate genetic data, remote sensing photos, uncertainty quantification, and lightweight model compression.

Author Contributions

Kateřina Svobodová contributes to conceptualization, methodology, software, validation, analysis, investigation, data collection, draft preparation, manuscript editing, visualization, supervision, project administration, and funding acquisition. Jiří Vaněk contributes to software, validation, analysis, investigation, data collection, draft preparation. All authors have read and agreed with the manuscript before its submission and publication.

Funding

This research received no specific financial support from any funding agency.

Institutional Review Board Statement

Not applicable.

References

[1] van Klompenburg, T., Kassahun, A., & Catal, C. (2020). Crop yield prediction using machine learning: A systematic literature review. Computers and Electronics in Agriculture, 177, 105709. https://doi.org/10.1016/j.compag.2020.105709

[2] Khaki, S., & Wang, L. (2019). Crop yield prediction using deep neural networks. Frontiers in Plant Science, 10, 621. https://doi.org/10.3389/fpls.2019.00621

[3] Nevavuori, P., Narra, N., & Lipping, T. (2019). Crop yield prediction with deep convolutional neural networks. Computers and Electronics in Agriculture, 163, 104859. https://doi.org/10.1016/j.compag.2019.104859

[4] Paudel, D., Boogaard, H., de Wit, A., Janssen, S., Osinga, S., Pylianidis, C., & Athanasiadis, I. N. (2021). Machine learning for large-scale crop yield forecasting. Agricultural Systems, 187, 103016. https://doi.org/10.1016/j.agsy.2020.103016

[5] Shahhosseini, M., Hu, G., Huber, I., & Archontoulis, S. V. (2021). Coupling machine learning and crop modeling improves crop yield prediction in the US Corn Belt. Scientific Reports, 11, 1606. https://doi.org/10.1038/s41598-020-80820-1

[6] Nevavuori, P., Narra, N., & Linna, P. (2020). Crop yield prediction using multitemporal UAV data and spatio-temporal deep learning models. Remote Sensing, 12(23), 4000. https://doi.org/10.3390/rs12234000

[7] Muruganantham, P., Wibowo, S., Grandhi, S., Samrat, N. H., & Islam, N. (2022). A systematic literature review on crop yield prediction with deep learning and remote sensing. Remote Sensing, 14(9), 1990. https://doi.org/10.3390/rs14091990

[8] Xie, Y., & Huang, J. (2021). Integration of a crop growth model and deep learning methods to improve satellite-based yield estimation of winter wheat in Henan Province, China. Remote Sensing, 13(21), 4372. https://doi.org/10.3390/rs13214372

[9] Mandal, D., & Rao, Y. S. (2020). SASYA: An integrated framework for crop biophysical parameter retrieval and within-season crop yield prediction with SAR remote sensing data. Remote Sensing Applications: Society and Environment, 20, 100366. https://doi.org/10.1016/j.rsase.2020.100366

[10] Nihar, A., Patel, N. R., & Danodia, A. (2022). Machine-learning-based regional yield forecasting for sugarcane crop in Uttar Pradesh, India. Journal of the Indian Society of Remote Sensing, 50, 1511-1523. https://doi.org/10.1007/s12524-022-01549-0

[11] Mahbub, M. (2020). A smart farming concept based on smart embedded electronics, internet of things and wireless sensor network. Internet of Things, 9, 100161. https://doi.org/10.1016/j.iot.2020.100161
[12] Citoni, B., Fioranelli, F., Imran, M. A., & Abbasi, Q. H. (2019). Internet of Things and LoRaWAN-enabled future smart farming. IEEE Internet of Things Magazine, 2(4), 14-19. https://doi.org/10.1109/IOTM.0001.1900043
[13] Hewamalage, H., Bergmeir, C., & Bandara, K. (2021). Recurrent neural networks for time series forecasting: Current status and future directions. International Journal of Forecasting, 37(1), 388-427. https://doi.org/10.1016/j.ijforecast.2020.06.008
[14] Torres, J. F., Hadjout, D., Sebaa, A., Martínez-Álvarez, F., & Troncoso, A. (2021). Deep learning for time series forecasting: A survey. Big Data, 9(1), 3-21. https://doi.org/10.1089/big.2020.0159
[15] Benidis, K., Rangapuram, S. S., Flunkert, V., Wang, Y., Maddix, D., Turkmen, C., et al. (2022). Deep learning for time series forecasting: Tutorial and literature survey. ACM Computing Surveys, 55(6), 1-36. https://doi.org/10.1145/3533382
[16] Lim, B., Arık, S. Ö., Loeff, N., & Pfister, T. (2021). Temporal fusion transformers for interpretable multi-horizon time series forecasting. International Journal of Forecasting, 37(4), 1748-1764. https://doi.org/10.1016/j.ijforecast.2021.03.012
[17] Zhou, H., Zhang, S., Peng, J., Zhang, S., Li, J., Xiong, H., & Zhang, W. (2021). Informer: Beyond efficient transformer for long sequence time-series forecasting. Proceedings of the AAAI Conference on Artificial Intelligence, 35(12), 11106-11115. https://doi.org/10.1609/aaai.v35i12.17325
[18] Wan, R., Tian, Y., Zhang, Y., Liu, Z., & Wang, N. (2022). A multivariate temporal convolutional attention network for time-series forecasting. Electronics, 11(10), 1516. https://doi.org/10.3390/electronics11101516
[19] Pantiskas, L., Verstoep, K., & Bal, H. (2020). Interpretable multivariate time series forecasting with temporal attention convolutional neural networks. 2020 IEEE Symposium Series on Computational Intelligence, 1687-1694. https://doi.org/10.1109/SSCI47803.2020.9308570
[20] Lin, T., Koprinska, I., & Rana, M. (2021). Temporal convolutional attention neural networks for time series forecasting. 2021 International Joint Conference on Neural Networks, 1-8. https://doi.org/10.1109/IJCNN52387.2021.9534351
[21] Barredo Arrieta, A., Díaz-Rodríguez, N., Del Ser, J., Bennetot, A., Tabik, S., Barbado, A., et al. (2020). Explainable Artificial Intelligence (XAI): Concepts, taxonomies, opportunities and challenges toward responsible AI. Information Fusion, 58, 82-115. https://doi.org/10.1016/j.inffus.2019.12.012
[22] Ryo, M. (2022). Explainable artificial intelligence and interpretable machine learning for agricultural data analysis. Artificial Intelligence in Agriculture, 6, 257-265. https://doi.org/10.1016/j.aiia.2022.11.003
[23] Apley, D. W., & Zhu, J. (2020). Visualizing the effects of predictor variables in black box supervised learning models. Journal of the Royal Statistical Society: Series B, 82(4), 1059-1086. https://doi.org/10.1111/rssb.12377
[24] Lundberg, S. M., Erion, G. G., Lee, S. I., & others. (2020). From local explanations to global understanding with explainable AI for trees. Nature Machine Intelligence, 2, 56-67. https://doi.org/10.1038/s42256-019-0138-9
[25] Tjoa, E., & Guan, C. (2021). A survey on explainable artificial intelligence (XAI): Toward medical XAI. IEEE Transactions on Neural Networks and Learning Systems, 32(11), 4793-4813. https://doi.org/10.1109/TNNLS.2020.3027314
[26] Mariadass, D. A., Moung, E. G., & Sufian, M. M. (2022). Extreme Gradient Boosting (XGBoost) regressor and Shapley additive explanation for crop yield prediction in agriculture. 2022 12th International Conference on Computer and Knowledge Engineering, 194-199. https://doi.org/10.1109/ICCKE57176.2022.9960069
[27] Yasaswy, K., Manimegalai, P., & Somasundaram, K. (2022). Crop yield prediction in agriculture using gradient boosting algorithm compared with random forest. 2022 International Conference on Cyber Resilience, 1-6. https://doi.org/10.1109/ICCR56254.2022.9995829
[28] Basha, S. M., Rajput, D. S., & J, V. (2020). Principles and practices of making agriculture sustainable: Crop yield prediction using random forest. Scalable Computing: Practice and Experience, 21(4), 591-600. https://doi.org/10.12694/scpe.v21i4.1714
[29] Saini, A., & Nagpal, C. K. (2022). Deep-LSTM model for wheat crop yield prediction in India. 2022 Fifth International Conference on Computational Intelligence and Communication Technologies, 120-125. https://doi.org/10.1109/CCICT56684.2022.00025

[30] Kuriakose, A., & Singh, P. (2022). Indian crop yield prediction using LSTM deep learning networks. 2022 13th International Conference on Computing Communication and Networking Technologies, 1-6. https://doi.org/10.1109/ICCCNT54827.2022.9984407

[31] Terliksiz, A. S., & Altylar, D. T. (2019). Use of deep neural networks for crop yield prediction: A case study of soybean yield in Lauderdale County, Alabama, USA. 2019 8th International Conference on Agro-Geoinformatics, 1-4. https://doi.org/10.1109/Agro-Geoinformatics.2019.8820257

[32] Wu, B., Wang, M., Jiang, C., & Li, Q. (2022). Crop yield estimation in the North China Plain from 2001 to 2016 using multi-source remote sensing data and process-based FGM model. ISPRS Annals of the Photogrammetry, Remote Sensing and Spatial Information Sciences, X-3/W2-2022, 43-50. https://doi.org/10.5194/isprs-annals-X-3-W2-2022-43-2022

[33] Shetty, A., & Smitha, N. (2021). Smart agriculture using IoT and machine learning. Transactions on Computer Systems and Networks, 1, 1-18. https://doi.org/10.1007/978-981-16-6124-2_1

[34] Sharma, A. (2021). Smart agriculture services using deep learning, big data, and IoT. In Smart Agriculture Services Using Deep Learning, Big Data, and IoT (pp. 220-245). IGI Global. https://doi.org/10.4018/978-1-7998-5003-8.ch010

[35] Ahmed, M., & Nabi, M. (2021). Machine learning (ML) driven agriculture. In Agriculture 5.0: Artificial Intelligence, IoT, and Machine Learning (pp. 119-140). CRC Press. https://doi.org/10.1201/9781003125433-6

[36] Ahmed, M., & Nabi, M. (2021). AI driven smart agriculture. In Agriculture 5.0: Artificial Intelligence, IoT, and Machine Learning (pp. 95-118). CRC Press. https://doi.org/10.1201/9781003125433-5

[37] Sharma, P., Jain, R., & Gupta, A. (2021). Deep learning approaches to time series forecasting. In Recent Advances in Time Series Forecasting (pp. 89-112). CRC Press. https://doi.org/10.1201/9781003102281-6

[38] Kumar, V., Srivastava, A., & Singh, R. (2022). Smart irrigation in farming using internet of things. In Smart Agriculture (pp. 167-184). CRC Press. https://doi.org/10.1201/b22627-10

[39] Wang, Y., Miao, Y., Dong, R., & Sun, Y. (2021). Improving in-season nitrogen status diagnosis using a three-band active canopy sensor and ancillary data with machine learning. In Precision Agriculture '21 (pp. 459-465). Wageningen Academic Publishers. https://doi.org/10.3920/978-90-8686-916-9_54

[40] Saha, K. (2020). Time series modelling and forecasting in agriculture: Basic to advanced. In Advanced Agriculture (pp. 171-188). New Delhi Publishers. https://doi.org/10.30954/ndp-advagr.2020.12